

Accurate Estimation of Solvation Free Energy Using Polynomial Fitting Techniques

Conrad Shyu
conrads@uidaho.edu

F. Marty Ytreberg
ytreberg@uidaho.edu

Department of Physics
University of Idaho
Moscow, ID 83844-0903

Department of Physics
University of Idaho
Moscow, ID 83844-0903

May 11, 2022

Abstract

This report details an approach to improve the accuracy and precision of free energy difference estimates using thermodynamic integration data (slope of the free energy with respect to the switching variable λ) and its application to calculating solvation free energy. The central idea is to utilize polynomial fitting schemes to approximate the thermodynamic integration data to improve the accuracy and precision of the free energy difference estimates. In this report we introduce polynomial and spline interpolation techniques. Two systems with analytically solvable relative free energies are used to test the accuracy and precision of the interpolation approach (Shyu and Ytreberg, *J Comput Chem* 30: 2297–2304, 2009). We also use both interpolation and extrapolation methods to determine a small molecule solvation free energy. Our simulations show that, using such polynomial techniques and non-equidistant λ values, the solvation free energy can be estimated with high accuracy without using soft-core scaling and separate simulations for Lennard-Jones and partial charges. The results from our study suggest these polynomial techniques, especially with use of non-equidistant λ values, improve the accuracy and precision for ΔF estimates without demanding additional simulations. To allow researchers to immediately utilize these methods, free software and documentation is provided via <http://www.phys.uidaho.edu/ytreberg/software>.

1 Introduction

The Helmholtz or Gibbs free energy constitutes an important thermodynamic quantity to understand how chemical species recognize each other, associate or react. Examples of such problems include conformational equilibria and molecular association, partitioning between immiscible liquids, receptor-drug interaction, protein-protein and protein-DNA association, and protein stability [1, 2]. Thermodynamic integration (TI) is a commonly used approach for the calculation of free energy differences (ΔF) between two systems with potential energy functions U_1 and U_0 , respectively [3, 4, 5, 6, 7]. The free energy difference, $\Delta F = F_1 - F_0$, is equivalent to

the reversible work to switch from U_0 to U_1 , and can be determined by estimating the integral

$$\Delta F = \int_{\lambda=0}^1 \left\langle \frac{\partial U_\lambda}{\partial \lambda} \right\rangle_\lambda d\lambda. \quad (1)$$

The notation $\langle \partial U_\lambda / \partial \lambda \rangle_\lambda$ indicates an ensemble average at a particular value of λ . The variable λ permits continuously switching from one energy function to another. Switching potential energies requires a continuously variable energy function U_λ such that $U_{\lambda=0} = U_0$ and $U_{\lambda=1} = U_1$. In addition, the free energy function U_λ must be differentiable with respect to λ for $0 \leq \lambda \leq 1$ [8].

The relationship in Equation 1 is exact. The numerical estimation comes into play because the integral must be approximated by performing simulations at various fixed, discrete, values of λ . Typically, these discrete λ values are used to convert the integral to a sum (e.g., using quadrature). If the estimate of $\langle \partial U_\lambda / \partial \lambda \rangle_\lambda$ is slow to converge, then it is necessary to perform very long simulations in order to reliably estimate the average. In addition, $\langle \partial U_\lambda / \partial \lambda \rangle_\lambda$ may heavily depend on λ so that a large number of fixed λ simulations is needed in order to estimate the integral with sufficient accuracy.

Previously, Shyu and Ytreberg [9] reported the use of regression techniques to calculate the free energy from TI data. Using analytical solvable examples, the authors were able to achieve highly accurate estimates. We note that regression does not produce a curve that goes through every data point exactly. Instead the regression model only describes the tendency of the data and does not represent the functional form.

The purpose of this current study is to introduce polynomial and spline interpolation techniques to estimate ΔF and to use both interpolation and regression methods to estimate a small molecule solvation free energy. This differs from our previous study in that these polynomials interpolate the slope of the free energy $dF/d\lambda = \langle \partial U_\lambda / \partial \lambda \rangle_\lambda$ as a function of λ . The derived curve is forced to pass through each data point. Regression, by contrast, constructs the curve that minimizes the errors between the data and extrapolated points. The key motivation for this study is that, even if the averages $\langle \partial U_\lambda / \partial \lambda \rangle_\lambda$ are fully converged (i.e., infinitely long sampling), there will be error in the ΔF estimates due to the fact that one must estimate the integral. Here we present methods which reduce this error and construct the polynomial that represents the functional form of TI data. We also examine the use of both equidistant and non-equidistant λ values. Two test systems previously used by Shyu and Ytreberg [9] with analytical ΔF values were utilized to quantify the accuracy and precision of the interpolation techniques. We also used both regression and interpolation techniques to estimate a small molecule solvation free energy. The results from our simulations suggest that polynomial fitting, especially with use of non-equidistant λ values, improves the accuracy and precision for ΔF estimates without demanding additional simulations. In addition, polynomial fitting techniques permit accurate estimates of free energy difference from TI without the need for soft-core scaling and separate simulations for partial charges and Lennard-Jones potentials.

2 Theory

The primary focus of this study is to present a mathematical framework for the analysis of fixed TI simulation data using polynomial and spline interpolation techniques. The objective is then to construct a polynomial that best fits the TI data. The functional form of the simulation data is represented by a series of data points $\{\lambda, dF/d\lambda\}$, thus a polynomial is constructed through these data. Interpolation refers to the problem of determining a function that exactly represents given data points. Mathematically the polynomial obtained from interpolation is considered to be the one that best represents all data points within the given interval ($\lambda = [0, 1]$) [10, 11].

Polynomial interpolation and regression techniques generally give a similar result, especially when high degrees of polynomials are employed to fit the TI data. However, the curve obtained from polynomial interpolation passes through each data point whereas the curve generated via regression does not. If TI simulations are fully converged (i.e., infinite sampling), then polynomial interpolation should give the most accurate and precise estimate. Regression, on the other hand, utilizes the least squares method that minimizes the sum of the square of the difference between the actual value and the approximated one. Regression does have an advantage over interpolation in that the approximation is independent of the number of data points. However, we note that regression may not give the best estimates if the TI data include several inflection points due to the fact that regression does not attempt to construct a curve that passes through every data point.

2.1 Mathematical Notation

To simplify the mathematical expressions and to be consistent with the most commonly used notation in polynomial and spline interpolation papers, we denote the switching variable λ by x , and, $dF/d\lambda$ by y . We also denote the actual continuous function $dF/d\lambda$ by $f(x)$. The functional form of the simulation data is thus represented by a series of data points $\{\lambda, dF/d\lambda\} = \{x, y\}$, and the approximating function $p(x)$ is constructed through these data points. The following sections briefly introduce mathematical definitions and properties of both Lagrange and Newton polynomials, and the cubic spline function.

2.2 Lagrange and Newton Polynomial Interpolation

The classical Weierstrass theorem establishes the mathematical foundation for polynomial approximation [12]. The theorem asserts that there exists a polynomial $p(x)$ for approximating the continuous function $f(x)$ defined within a closed interval $[a, b] = [0, 1]$, and the polynomial approximation $p(x)$ can get arbitrarily close to the function $f(x)$ as the degree of polynomial is increased [13]. The most straightforward method to obtain the polynomial $p(x)$ of degree n is to calculate the values of $f(x)$ for $n+1$ distinct fitting data points within the interval of $a \leq x \leq b$, and satisfy the simultaneous equation $y_i = f(x_i) = p(x_i)$, for $i = 0, 1, 2, \dots, n$. Lagrange and Newton polynomials are the most commonly used methods for interpolation [13, 15].

The coefficients of the above polynomial $p(x)$ then form the basis of the Lagrange interpolation formula. The Weierstrass theorem contends that there is always a unique polynomial

$p(x)$ of degree n that satisfies these conditions. The Lagrange interpolation polynomial $L(x)$ is a linear combination of Lagrange basis polynomials $l_i(x)$ such that

$$L(x) = \sum_{i=0}^n y_i l_i(x) = \sum_{i=0}^n y_i \left[\prod_{\substack{j=0 \\ j \neq i}}^n \frac{x - x_j}{x_i - x_j} \right]. \quad (2)$$

It is worth noting that the degree of polynomial n cannot be chosen arbitrarily but is determined by the number of data points $n + 1$. This is important since the degree of interpolating polynomials will thus be determined by the number of λ values used to estimate ΔF .

Mathematically, the Lagrange form of the interpolation polynomial is generally preferred in proof and theoretical arguments because the derivatives of the polynomial are continuous, and maxima or minima always exist [10, 11]. The construction of Lagrange polynomials, however, is computationally demanding because all Lagrange basis polynomials have to be reevaluated each time y_i is updated. By contrast, Newton interpolation utilizes the divided difference (more on this below) which is generally more computationally efficient [14].

A more practical form of interpolation polynomial for computational purposes is given by Newton polynomials that utilize the divided difference. The divided difference is defined as the ratio of the difference in the function values, y_i or $f(x_i)$, at two points divided by the difference in the values of the corresponding independent variable, x_i . Divided differences do not require the recalculations of coefficients if new data points are included. As a consequence, it is generally more computationally efficient to use the divided differences method for interpolation [15]. Similar to the Lagrange polynomial, the Newton polynomial is a linear combination of basis polynomials

$$N(x) = \sum_{i=0}^n a_i \left[\prod_{j=0}^{i-1} (x - x_j) \right], \quad (3)$$

where the coefficients $a_i = g[x_0, \dots, x_i]$ is the notation for divided differences. The first divided difference, for example, between data points x_0 and x_1 is given by

$$a_1 = g[x_0, x_1] = \frac{f(x_1) - f(x_0)}{x_1 - x_0} = \frac{y_1 - y_0}{x_1 - x_0}. \quad (4)$$

The second divided difference between data points x_0 , x_1 , and x_2 is given by

$$a_2 = g[x_0, x_1, x_2] = \frac{g[x_1, x_2] - g[x_0, x_1]}{x_2 - x_0}. \quad (5)$$

Accordingly the n -th divided difference between data points x_0, x_1, \dots, x_n is given by

$$a_n = g[x_0, x_1, \dots, x_n] = \frac{g[x_1, x_2, \dots, x_n] - g[x_0, x_1, \dots, x_{n-1}]}{x_n - x_0}. \quad (6)$$

The Newton interpolation polynomial is then given by

$$\begin{aligned} N(x) = & f(x_0) + g[x_0, x_1](x - x_0) + g[x_0, x_1, x_2](x - x_0)(x - x_1) + \\ & \dots + g[x_0, x_1, \dots, x_i](x - x_0)(x - x_1) \dots (x - x_{i-1}). \end{aligned} \quad (7)$$

The calculations of the divided differences form a successive, recurrent relationship between the previous two coefficients. Computationally, the divided differences can be written in the form of a table that significantly simplifies the algorithmic implementation [15].

2.3 Spline Function Interpolation

Studies have suggested that the spline function is typically preferred over polynomials because the interpolation error can be reduced by using low degrees of polynomials [16, 17, 18]. Spline interpolation also avoids the Runge's phenomenon which occurs when using high degree polynomials [19]. Runge's phenomenon is when approximation errors increase dramatically as the degree of interpolation polynomials increases.

Spline functions are piecewise polynomials of the same degree [17, 20]. Unlike the Lagrange and Newton interpolation polynomials, the degree of the piecewise polynomials does not depend on the number of data points. The piecewise polynomials join together at the data points $\{\lambda, dF/d\lambda\}$ called knots and must be continuous [10]. The main advantages of spline interpolation are stability and simplicity [21]. Moreover, the use of polynomials of lower degree offers the possibility to avoid the oscillatory behavior that commonly arises from fitting a single polynomial exactly to a large number of data points [10].

We utilize the cubic spline which is the most commonly used type. A cubic spline function is a set of third degree piecewise polynomials that provide a smooth curve passing through all data points. Because the segments join with matching derivatives up to order two, the curvature of the polynomials changes smoothly along the knots. The fundamental idea behind cubic spline interpolation is based on the engineer's tool used to draw smooth curves through a number of points. This spline consists of weights attached to a flat surface at the points to be connected. A flexible strip is then bent across each of these weights, resulting in a smooth curve. The mathematical spline is similar in principle. The points, in this case, are TI data. The weights are the coefficients of the cubic polynomials used to interpolate the data [22].

Mathematically, the cubic spline function $S_i(x)$ is defined as

$$S_i(x) = \frac{z_{i+1}}{6h_i}(x-x_i)^3 + \frac{z_i}{6h_i}(x_{i+1}-x)^3 + \left(\frac{y_{i+1}}{h_i} - \frac{h_i}{6}z_{i+1}\right)(x-x_i) + \left(\frac{y_i}{h_i} - \frac{h_i}{6}z_i\right)(x_{i+1}-x), \quad (8)$$

where $h_i = x_{i+1} - x_i$ is the size of the i -th interval $[x_i, x_{i+1}]$. The spline function $S_i(x)$ provides a cubic polynomial on the interval $x \in [x_i, x_{i+1}]$. The values of z_i are the second derivatives at the the endpoints such that $z_i = S_i''(x_i)$. To compute the values of z_i , it is necessary to solve the recurrent equation

$$h_{i-1}z_{i-1} + 2(h_{i-1} + h_i)z_i + h_i z_{i+1} = 6 \left(\frac{y_{i+1} - y_i}{h_i} - \frac{y_i - y_{i+1}}{h_{i-1}} \right), \quad (9)$$

for $i = 0$ to $n - 1$.

In the current study, natural spline boundary conditions were implemented to construct the interpolation polynomials. There are two boundary condition types which could be utilized. The natural cubic spline imposes the boundary conditions $z_0 = 0$ and $z_n = 0$, and the clamped cubic spline requires z_0 and z_n for a given function [16, 17]. When the natural boundary conditions are used, the spline assumes the shape that a long flexible curve would take if it is forced to go through all the data points. A natural spline permits the slope at the ends be free to equilibrate to the position that minimizes the oscillatory behavior of the curve. A clamped

cubic spline, on the other hand, further requires a piecewise cubic function which passes through the given set of knots with a given function or value. The derivatives and second derivatives of adjacent cubic polynomials must also agree at the interior abscissae. It is worth noting that spline interpolation polynomials are piecewise and do not always approximate the $dF/d\lambda$ completely. This is particularly evident when the choice of λ neglects the inflection points along the curve.

2.4 Algebraic Formulation

To minimize the numerical errors in the ΔF estimation process, interpolating polynomials were first transformed into their analytical forms, and then all integrals were evaluated analytically. The derivation of the analytical integration form for the interpolating polynomials involves the expansion of every coefficient in the polynomial equation. The rearrangement of coefficients permits analytical integration of the interpolating polynomials. The analytical integral for the Lagrange polynomial is expressed as

$$\int L(x) dx = \sum_{i=0}^n y_i \int l_i(x) dx = \sum_{i=0}^n y_i \int \prod_{i \neq j, j=0}^n \frac{x - x_j}{x_i - x_j} dx. \quad (10)$$

Similarly, the analytical integral for the Newton polynomial is expressed as

$$\int N(x) dx = \sum_{i=0}^n a_i \int \prod_{j=0}^{i-1} (x - x_j) dx, \quad (11)$$

where the coefficient a_i is the notation for divided differences; see Equation 3.

For spline functions, analytical integrations must be performed at each subinterval. Similar to that of Lagrange and Newton polynomial, the integration form requires the expansion and rearrangement of all coefficients. The analytical integral form of the cubic spline is expressed as

$$\begin{aligned} \int S_i(x) dx &= x^3 \left[\frac{1}{6h_i} (z_{i+1} - z_i) \right] + x^2 \left[\frac{1}{2h_i} (z_i x_{i+1} - z_{i+1} x_i) \right] + \\ &x \left[\frac{1}{2h_i} (z_{i+1} x_i^2 - z_i x_{i+1}^2) + \frac{1}{h_i} (y_{i+1} - y_i) - \frac{h_i}{6} (z_{i+1} - z_i) \right] + \\ &\frac{1}{6h_i} (z_i x_{i+1}^3 - z_{i+1} x_i^3) + \frac{1}{h_i} (y_i x_{i+1} - y_{i+1} x_i) + \frac{h_i}{6} (z_{i+1} x_i - z_i x_{i+1}). \end{aligned} \quad (12)$$

Similar to that of Lagrange and Newton interpolation polynomials, each x_i is replaced by λ_i and y_i by $\langle \partial U_\lambda / \partial \lambda \rangle_{\lambda_i}$. Specifically, for Lagrange interpolation

$$\Delta F = \int_0^1 L(\lambda) d\lambda = \sum_{i=0}^n \left\langle \frac{\partial U_\lambda}{\partial \lambda} \right\rangle_{\lambda_i} \int_0^1 \prod_{i \neq j, j=0}^n \frac{\lambda - \lambda_j}{\lambda_i - \lambda_j} d\lambda \quad (\text{Lagrange}) \quad (13)$$

and for Newton interpolation

$$\Delta F = \int_0^1 N(\lambda) d\lambda = \sum_{i=0}^n a_i \int_0^1 \prod_{j=0}^{i-1} (\lambda - \lambda_j) d\lambda \quad (\text{Newton}) \quad (14)$$

with the divided difference $a_i = g[\lambda_0, \lambda_1, \dots, \lambda_i]$ given by Equation 6. To calculate ΔF using cubic spline, integrals are evaluated at each subinterval $[\lambda_{i-1}, \lambda_i]$, and the total ΔF is the sum of all integrals

$$\Delta F = \sum_{i=1}^n \int_{\lambda_{i-1}}^{\lambda_i} S_i(\lambda) d\lambda \quad (\text{Cubic Spline}) \quad (15)$$

where S_i are given by Equation 8.

3 Computational Details

Two types of free energy calculations were performed in order to test our interpolation approaches. The first type utilized two test systems with analytical ΔF solutions [9]. Simulations were performed using the same protocols as reported by Shyu and Ytreberg [9]. These test systems provide an unbiased measure of the accuracy and precision of the interpolation techniques for estimating ΔF .

The second type of simulation was to compute the solvation free energy for a 4-hydroxy-2-butanone (BUQ) molecule [26]. We used both regression [9] and interpolation techniques and compared them to use of quadrature. Details of the solvation free energy calculation are described below.

3.1 Test Systems

Procedures for the simulations of the two test systems were previously described by Shyu and Ytreberg [9]. Briefly, these systems involve two potential functions $U_0(\xi) = \frac{1}{2}\xi^2$ and $U_1(\xi) = 2(\xi - 5)^2$ for system one, and $U_0(\xi) = \frac{5}{2}\xi^2$ and $U_1(\xi) = \frac{1}{2}(\xi - 5)^2$ for system two with the analytical free energy $\Delta F = -\frac{1}{2} \ln \frac{1}{4}$ and $\Delta F = -\frac{1}{2} \ln 5$ respectively [9]. An equal amount of simulation time (1,000,000 Monte Carlo steps) was spent for each of six ($\lambda = 0.0, 0.2, 0.4, 0.6, 0.8,$ and 1.0) and eleven ($\lambda = 0.0, 0.1, 0.2, \dots, 0.9,$ and 1.0) equidistant λ values. Identical equilibrium simulations were performed on the corresponding six non-equidistant λ values ($\lambda = 0.0, 0.0955, 0.3455, 0.6545, 0.9045,$ and 1.0) and eleven ($\lambda = 0.0, 0.0245, 0.0955, 0.2061, 0.3455, 0.5, 0.6545, 0.7939, 0.9045, 0.9755,$ and 1.0). Averages of the slope $dF/d\lambda = \langle \partial U_\lambda / \partial \lambda \rangle_\lambda$ were collected for each value of λ . For each λ value, simulations were given 1,000 steps to equilibrate initially, then were allowed to proceed for 1,000,000 Monte Carlo steps. Each trial started with an arbitrarily chosen initial position for the particle. Simulations were performed sequentially starting at $\lambda = 0$. Trial moves for Metropolis Monte Carlo [25] were generated by adding a uniform random deviate between -0.5 and 0.5 to the current position resulting in a 40 to 50% acceptance ratio. A total of 1,000 independent trials were generated from each case. We recorded the biases ($\Delta F_{\text{exact}} - \Delta F_{\text{estimate}}$) for each of 1,000 independent runs and the corresponding averages and standard deviations were calculated in order to provide a measure of the accuracy and precision of the ΔF estimates.

3.2 BUQ Solvation

We applied our interpolation technique to compute the solvation free energy for a BUQ molecule [26]. We first obtained a reference estimate for the solvation free energy ΔF_{ref} . To obtain ΔF_{ref} with high accuracy, we performed separate simulations for changes in the Lennard-Jones parameters and the partial charges [27]. Studies have shown that use of separate simulations provides a higher accuracy estimate and avoids possible endpoint singularity problems [6, 27, 28]. Thus, the first stage to obtaining ΔF_{ref} was to compute the free energy associated with the Lennard-Jones potential. This was accomplished by setting all the partial charges of the solute to zero. We then “grew” the BUQ molecule in the solvent using soft-core scaling to ensure a smooth potential energy curve, even for interpenetrating molecules [28, 29]. Once the neutral atoms are fully grown in the solvent, we performed the second stage to compute the free energy associated with the partial charges. This was accomplished by increasing the partial charges from zero to their final values given by the forcefield. For both stages, we employed trapezoidal quadrature to integrate the free energy slope and obtain the free energy for each of the two stages. We computed ΔF_{ref} using this two-stage approach for both inserting and deleting BUQ.

The initial coordinates for the BUQ were extracted from the FKBP-ligand complexes (1D7J) [26] which were retrieved from the Protein Data Bank. The topologies for BUQ were then generated by the PRODRG server [30]. The simulations were performed using the GROMACS package 3.3.3 [31] at constant temperature in a periodic cubic box with an edge length of approximately 2.4 nm and the default GROMOS-96 43A1 forcefield. This corresponded to approximately 500 SPC [32] water molecules. The neighbor list for nonbounded interactions was updated every 10 steps. The bond distances and bond angles of water were constrained using the LINCS algorithm [33]. To obtain an isothermal-isobaric ensemble at 300 K, a leap-frog stochastic dynamics [34] was used to integrate the equations of motion with a 2.0 fs timestep. The temperature was maintained using Langevin dynamics with a friction coefficient of 1.0 amu/ps. The pressure was maintained at 1.0 atom using the Parrinello-Rahman algorithm [35]. The coupling time was set to 1.0 ps, and the isothermal compressibility was set to 4.5×10^{-5} bar⁻¹. Particle-mesh summation Ewald algorithm [36, 37] was used for electrostatics with a real-space cutoff of 1.0 nm and a Fourier spacing of 0.1 nm. Van der Waals interactions used a cutoff with a smoothing function such that the interactions smoothly decayed to zero between 0.75 nm and 0.9 nm. Dispersion corrections for the energy and pressure were also utilized [38].

The BUQ system was first minimized using steepest descent for 500 steps. 100 ps of constant volume simulation were performed for system equilibration, followed by 100 ps of constant pressure simulation. Then 10 ns constant pressure simulations were performed with eleven equidistant λ values ($\lambda = 0.0, 0.1, 0.2, \dots, 0.9$, and 1.0). Simulations were performed sequentially starting at $\lambda = 0$ and averages of the slope $dF/d\lambda = \langle \partial U_\lambda / \partial \lambda \rangle_\lambda$ were collected for each value of λ . For the first stage, we computed the free energy for the Lennard-Jones interactions using a soft-core scaling parameter of $\alpha = 0.5$. For the second stage, we computed the free energy for the partial charge interactions using $\alpha = 0.0$ [27]. Four additional λ values ($\lambda = 0.65, 0.75, 0.85, 0.95$ for deleting BUQ and $\lambda = 0.05, 0.15, 0.25, 0.35$ for inserting) were included to the simulations for Lennard-Jones potentials to further refine the ΔF soft-core estimate where the free energy slopes undergo the most change. The total free energy is the sum

of the free energies from simulations for the Lennard-Jones and partial charges. We determined that $\Delta F_{\text{ref}}^{\text{del}} = 31.6$ kJ/mol for deleting BUQ and $\Delta F_{\text{ref}}^{\text{ins}} = -31.5$ kJ/mol for inserting.

4 Results and Discussion

We now summarize the results from our polynomial fitting methods applied to two test systems, and to BUQ solvation. The analytical test systems provide an objective assessment of the accuracy and precision of the ΔF estimates. The BUQ solvation provides a demonstration of our approach on a common chemical problem. For the results below, interpolation polynomials for each set of TI data were first transformed into the analytical form (Equations 13, 14, and 15) and integration was then performed analytically. Results presented below show that use of interpolation with non-equidistant λ values results in accurate and precise ΔF estimates.

4.1 Test Systems

Table 1 summarizes the averages and standard deviations of biases for system one and two from 1,000 independent trials using six and eleven equidistant and non-equidistant λ values. Using equidistant λ values, the estimates obtained from the cubic spline and trapezoidal quadrature are both heavily biased. As the number of λ values increases, the accuracy and precision improve. Using eleven equidistant λ values, for example, the Lagrange and Newton polynomials give the most accurate estimates of ΔF but with large uncertainty compared to that of the cubic spline and trapezoidal quadrature. The estimates obtained from cubic spline are slightly biased but with a low uncertainty. Using non-equidistant λ values, the Lagrange and Newton polynomials are able to most accurately estimate ΔF . These results suggest that using non-equidistant λ values is preferred to equidistant λ values. Quadrature results, however, do not improve with the use of non-equidistant λ values. We also note that, unlike quadrature, the steep free energy curvature for system two does not appear to significantly decrease the accuracy of ΔF estimates obtained from the Lagrange and Newton polynomials. These results are consistent with our previous regression study [9].

Overall, the Lagrange and Newton polynomials provide the most accurate estimates, but often with larger uncertainty than that of spline or quadrature. Results from additional cursory simulations suggest that the variation of the ΔF estimates are predominately caused by the oscillations from the use of high degree polynomials (data not shown). Use of non-equidistant λ values significantly improves the numerical stability and increases the accuracy and precision of ΔF estimates when using polynomial interpolation. The use of non-equidistant λ values, however, provides only slight improvement of the estimates obtained from the trapezoidal quadrature compared to that of equidistant. The results also show that the ΔF estimates obtained from spline interpolation are more accurate than that of trapezoidal rule. The estimates from quadrature are all heavily biased. The estimates from the cubic spline have similar uncertainty but are not as accurate as that of Lagrange and Newton. Thus, we conclude that use of both polynomial and spline interpolation techniques with non-equidistant λ values provide accurate estimates of ΔF .

System One [9]				
	Six Equid.	Six Non-Equid.	Eleven Equid.	Eleven Non-Equid.
Trapezoidal Rule	1.2496 (0.0210)	1.1390 (0.0212)	0.3270 (0.0152)	0.3073 (0.0150)
Cubic Spline	0.4686 (0.0198)	-0.1138 (0.0218)	0.0752 (0.0152)	-0.0047 (0.0152)
Lagrange/Newton	0.1606 (0.0200)	-0.0208 (0.0212)	0.0034 (0.0377)	0.0006 (0.0151)
System Two [9]				
	Six Equid.	Six Non-Equid.	Eleven Equid.	Eleven Non-Equid.
Trapezoidal Rule	-1.8944 (0.0232)	-1.4944 (0.0231)	-0.5077 (0.0161)	-0.4094 (0.0154)
Cubic Spline	-0.8228 (0.0212)	0.2035 (0.0234)	-0.1424 (0.0159)	0.0093 (0.0156)
Lagrange/Newton	-0.3495 (0.0210)	0.0467 (0.0227)	-0.0053 (0.0335)	-0.0006 (0.0154)

Table 1: Averages and standard deviations of the biases ($\Delta F_{\text{exact}} - \Delta F_{\text{estimate}}$) for system one and two using six and eleven equidistant and non-equidistant λ values. The exact solution for system one is $\Delta F_{\text{exact}}^{\text{one}} = -\frac{1}{2} \ln \frac{1}{4}$ and for system two $\Delta F_{\text{exact}}^{\text{two}} = -\frac{1}{2} \ln 5$ as previously reported by Shyu and Ytreberg [9]. Standard deviations of the biases are shown in parentheses.

	Del. Equid.	Del. Non-Equid.	Ins. Equid.	Ins. Non-Equid.
Trapezoidal Rule	-40.2	-9.5	39.6	9.5
Cubic Spline	-26.8	1.0	27.0	-1.1
Lagrange/Newton	-14.0	-0.4	14.5	0.4
Regression [9]	-14.3	-0.4	14.5	0.3

Table 2: Free energy biases ($\Delta F_{\text{ref}} - \Delta F_{\text{estimate}}$) using eleven equidistant and non-equidistant λ values. The reference free energy estimates ($\Delta F_{\text{ref}}^{\text{del}}$ and $\Delta F_{\text{ref}}^{\text{ins}}$) were obtained from a two-stage simulation using soft-core scaling and are utilized as reference values to evaluate the polynomial techniques. The free energy for BUQ deletion is $\Delta F_{\text{ref}}^{\text{del}} = 31.6$ kJ/mol and insertion $\Delta F_{\text{ref}}^{\text{ins}} = -31.5$ kJ/mol.

4.2 BUQ Solvation

As detailed above, we first performed a two-stage simulation for Lennard-Jones and partial charges in order to obtain the reference solvation free energies $\Delta F_{\text{ref}}^{\text{ins}}$ and $\Delta F_{\text{ref}}^{\text{del}}$. We then determined the free energy estimate with no soft-core scaling utilizing a single stage, i.e., Lennard-Jones and partial charges were simultaneously changed. Figure 1 shows the free energy curves from the simulations using eleven equidistant (b) and non-equidistant λ values (a). The curves are all well-behaved except when λ is close to either 0.0 or 1.0. As expected, the figures show clear evidence of the endpoint singularity when the vanishing or growing atoms become close to the other atoms. The statistical uncertainty progressively grows larger as λ approaches 0.0 or 1.0. The rapid changes on the free energy curves at the endpoint introduce significant errors into the numerical integration using trapezoid quadrature. It is worth noting that the use of non-equidistant λ significantly alleviates the endpoint singularity problem, even for quadrature, because more data points are used at each end.

Table 2 summarizes the ΔF estimates obtained using both interpolation and regression

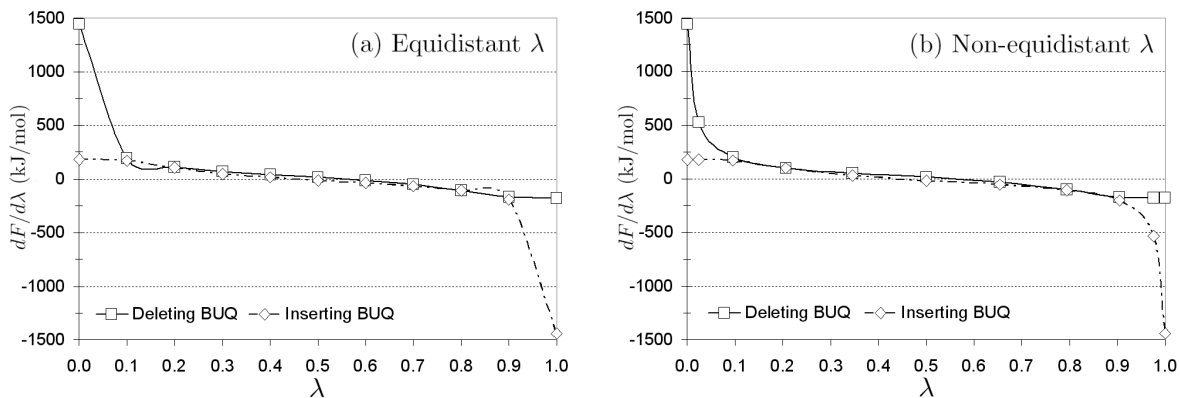


Figure 1: Solvation free energy curves for BUQ with eleven equidistant (a) and non-equidistant (b) λ values. Both insertion (solid curve) and deletion (dotted curve) were computed. The fitting curves shown were constructed using Lagrange interpolating polynomials. Note that the endpoint singularity problem is present when the growing and vanishing atoms are too close to the other atoms ($\lambda = 0.0$ or 1.0). The use of non-equidistant λ values allows a smoother polynomial fit.

techniques with equidistant (Table 2A) and non-equidistant λ values (Table 2B). The reference free energies $\Delta F_{\text{ref}}^{\text{ins}}$ and $\Delta F_{\text{ref}}^{\text{ins}}$ were used to estimate the accuracy and precision of these polynomial fitting techniques. For equidistant λ values, while none of the integration techniques give an accurate estimate of ΔF , Lagrange and Newton provide the best results. The use of non-equidistant λ values, significantly improves the accuracy of all ΔF estimates. The improvement is particularly evident with the estimates obtained using Lagrange and Newton polynomials. Cubic spline interpolation delivers slightly biased estimates but is still considerably more accurate than that of trapezoidal quadrature.

For BUQ solvation, our study has shown that using the polynomial fitting techniques for interpolation and extrapolation and use of non-equidistant λ values, ΔF can be estimated within the accuracy of ± 0.4 kJ/mol *without using soft-core scaling and performing separate simulations for Lennard-Jones or partial charges*. Steinbrecher et al. [27] showed that the soft-core potentials are most promising for alchemical TI simulations and deliver ΔF estimates with accuracies of 0.1 kcal/mol. However, our simulations suggest that similar accuracy can be achieved using non-equidistant λ values and polynomial fitting techniques without soft-core scaling.

5 Conclusion

We have implemented polynomial interpolation and regression techniques to estimate a small molecule solvation free energy using thermodynamic integration (TI) simulation data. Our study utilized two test systems with analytical ΔF values to objectively quantify the accuracy and precision of the interpolation techniques. We also used both interpolation and regression to estimate the solvation free energy for BUQ. These polynomial approaches rely on constructing

globally optimal polynomials that best fit the TI data, which are then used to estimate ΔF . Additional algebraic calculations are done to permit analytical integration eliminating potential errors due to numerical evaluation on the integral.

Studies have shown that the use of soft-core scaling improves the accuracy of ΔF estimates within ± 0.1 kJ/mol for alchemical TI simulations [27]. Our simulations, however, suggest that similar accuracy can also be achieved using non-equidistant λ and polynomial interpolation or regression techniques without soft-core scaling.

We have shown that polynomial and spline interpolation techniques provide more accurate and precise ΔF estimates than trapezoidal quadrature for the systems studied here. However, we caution that polynomial interpolation techniques possess some inherent weakness. The most significant is that use of more than eleven λ produces interpolation polynomials that are numerically unstable. As a consequence, our approach is limited to use of eleven or less equidistant or non-equidistant λ values or one may judiciously select subsets of the λ data that best represent the underlying functional form of the free energy curve.

Our results also illustrate the importance of selection of λ values if one wishes to use polynomial interpolation techniques to improve the accuracy of ΔF estimates. For the systems studied here, use of non-equidistant λ always produced more accurate ΔF estimates than use of equidistant λ . Using twelve or less λ values the Lagrange and Newton polynomials always produced the highest accuracy. The ΔF estimates via cubic spline were more accurate than quadrature but less accurate than Lagrange and Newton. We note that for data containing more twelve λ values, cubic spline is expected to produce more accurate results than Lagrange and Newton because of superior numerical stability.

To better facilitate the use of polynomial fitting techniques, we propose several guidelines for estimating ΔF . Researchers who already have very well converged TI data with eleven or less λ values are encouraged to utilize the Lagrange or Newton polynomial interpolation approach. For researchers who already have data from equilibrium simulations with twelve or more λ values, the spline interpolation technique should be used instead. Researchers that have not yet generated data are strongly encouraged to use non-equidistant λ values and polynomial fitting techniques. Finally, if the TI data is noisy or not very well converged then regression [9] should be used instead of interpolation. To allow researchers to immediately utilize these methods, free software and documentation is provided via <http://www.phys.uidaho.edu/ytreberg/software>.

Acknowledgements

This research was supported by Idaho NSF-EPSCoR, Bionanoscience at University of Idaho (BANTech), and the Initiative for Bioinformatics and Evolutionary Studies (IBEST) at University of Idaho.

References

- [1] Chipot, C. and Pohorille, A. *Free energy calculations*. Springer, New York, NY, (2007).

- [2] Reddy, M. and Erion, M. *Free energy calculations in rational drug design*. Kluwer Academic/Plenum Publishers, New York, NY, (2001).
- [3] Kirkwood, J. *Journal of Chemical Physics* **3**, 300–313 (1935).
- [4] Mordasini, T. and McCammon, J. *Journal of Physical Chemistry B* **104**, 360–367 (2000).
- [5] Shirts, M. and Pande, V. *Journal of Chemical Physics* **122**, 144107 (2005).
- [6] Shirts, M., Pitner, J., Swope, W., and Pande, V. *Journal of Chemical Physics* **119**, 5740 (2003).
- [7] Ytreberg, F., Swendsen, R., and Zuckerman, D. *Journal of Chemical Physics* **125**, 1–11 (2006).
- [8] Leech, A. *Molecular modeling, principle and applications*. Pearson Education Limited, Harlow, Essex, UK, 2nd edition, (2001).
- [9] Shyu, C. and Ytreberg, F. *Journal of Computational Chemistry* **30**, 2297–2304 (2009).
- [10] Faires, J. and Burden, R. *Numerical methods*. PWS-Kent Publishing Company, Boston, MA, (1993).
- [11] Henry, M. *The American Mathematical Monthly* **91**, 497–499 (1981).
- [12] Bishop, E. *Pacific Journal of Mathematics* **11**, 777–783 (1961).
- [13] Jeffreys, H. and Jeffreys, B. *Lagrange’s interpolation formula*. Methods of mathematical physics. Cambridge University Press, Cambridge, England, 3rd edition, (1988).
- [14] Lee, E. *The American Mathematical Monthly* **96**, 618–622 (1999).
- [15] Werner, W. *Mathematics of Computation* **43**, 205–217 (1984).
- [16] Ahlberg, L., Nilson, E., and Walsh, J. *The theory of splines and their applications*. Academic Press, New York, (1967).
- [17] Greville, T. *Theory and applications of spline functions*. Academic Press, New York, (1969).
- [18] Schultz, M. *Mathematics of Computation* **24**, 507–515 (1970).
- [19] Epperson, J. *The American Mathematical Monthly* **94**, 329–341 (1987).
- [20] Boor, C. D. *A practical guide to splines*. Springer-Verlag, New York, NY, (1978).
- [21] Wold, S. *Technometrics* **16**, 1–11 (1974).
- [22] Schultz, M. *Spline analysis*. Prentice Hall, Englewood Cliffs, NJ, (1973).
- [23] Zelmer, G. *SIAM Review* **19**, 1–4 (1977).
- [24] Süli, E. and Mayers, D. *An introduction to numerical analysis*. Cambridge University Press, Cambridge, UK, (2003).

- [25] Metropolis, N, Rosenbluth, A.W., Rosenbluth, M.N., Teller, A.H. and Teller, E. *Journal of Chemical Physics* **21**, 1087–1092 (1953).
- [26] Burkhard, P., Taylor, P., and Walkinshaw, M. *Journal of Molecular Biology* **295**, 953–962 (2000).
- [27] Steinbrecher, T., Mobley, D., and Case, D. *Journal of Chemical Physics* **127**, 214108 (2007).
- [28] Zacharias, M., Straatsma, T., and McCammon, J. *Journal of Chemical Physics* **100**, 9025 (1994).
- [29] Beulter, T., Mark, A., van Schaik, R., Gerber, P., and van Gunsteren, W. *Chemical Physics Letters* **222**, 529–539 (1994).
- [30] Schüttelkopf, A. and van Aalten, D. *Acta Crystallographica* **D60**, 1355–1363 (2004).
- [31] Lindahl, E., Hess, B., and van der Spoel, D. *Journal of Molecular Modeling* **7**, 306–317 (2001).
- [32] Robinson, G., Zhu, S., Sigh, S., and Evans, M. *Water in biology, chemistry and physics: experimental overviews and computational methodologies*. World Scientific, Singapore, (1996).
- [33] Hess, B., Bekker, H., Berendsen, H., and Fraaije, J. *Journal of Computational Chemistry* **18**, 1463 (1997).
- [34] van Gunsteren, W. and Berendsen, H. *Molecular Simulation* **1**, 173–185 (1988).
- [35] Parrinello, M. and Rahman, A. *Physical Review Letters* **45**, 1196–1199 (1980).
- [36] Darden, T., York, D., and Pedersen, L. *Journal of Chemical Physics* **98**, 10089 (1993).
- [37] Essmann, U., Perera, L., Berkowitz, M., Darden, T., Lee, H., and Pedersen, G. *Journal of Computational Physics* **103**, 8577 (1995).
- [38] Allen, M. and Tildesley, D. *Computer simulation of liquids*. Oxford University Press, Oxford, UK, (1989).